International Journal of Applied Engineering Research
ISSN 0973-4562 Volume 9, Number 21 (2014) pp. 11631-11646

http://www.ripublication.com

Optical and Surface Properties of Zinc Oxide Nanoparticles Dried by Conventional and Supercritical Ethanol Drying Techniques

Theresa Obiajulu Egbuchunam[1,*], Senem Yetgin[2], Filiz Ozmihci Omurlu[2] and Devrim Balkose[2]

[1] Department of Chemistry, Federal University of Petroleum Resources Effurun, Delta State, Nigeria
[2] Department of Chemical Engineering, Izmir Institute of Technology 35430 Gulbahce Urla Izmir Turkey
Corresponding author: Theresa Obiajulu Egbuchunam, Ph.D, Associate Professor, research fields: materials, pollution management and control.
E-mail: tessychunam@gmail.com

Abstract

Zinc oxide (ZnO) nanoparticles were synthesized by conventional (ZnO-A) and supercritical ethanol drying (ZnO-B). Nitrogen adsorption/desorption analyses were performed to determine the surface areas of the powders. The specific surface area was 28.30m^2/g and 10.61 m^2/g for ZnO-A and ZnO-B respectively. The powders adsorbed very small amount of $CO_2$with the conventionally dried powder adsorbing more CO_2. Supercritical ethanol dried ZnO had ethanol on its surface which was eliminated by vacuum application at room temperature. Both powders had OH groups which were eliminated on heating up to 500^oC under vacuum. However, OH groups were present in lower amounts in supercritical ethanol dried ZnO. The powders were characterized by UV-VIS optical absorption and room temperature photoluminescence spectroscopic analyses. The UV-VIS absorption spectrum showed an absorption band at 375nm due to ZnO nanoparticles. The photoluminescence spectrum of ZnO excited at 380nm exhibited three emission peaks: one at 424nm and 490nm corresponding to band gap excitonic emission and another located at 520nm due to the presence of singly ionized oxygen vacancies.

Key words: Zinc oxide nanoparticles, *in situ* drift FTIR spectroscopy, supercritical ethanol drying, nitrogen and carbon dioxide adsorption, Luminescence

1. Introduction

Nanosized zinc oxide (ZnO) is a promising non-toxic, chemically stable semi-conductor material used for a variety of applications [1-6]. During production, nanoparticles agglomerate owing to the influence of interfacial tension during conventional drying [6-7]. In order to prevent particle agglomeration, a number of synthetic strategies have been developed to generate well-defined nanoparticles having structures and properties suitable for applications in aqueous and non-aqueous systems.

Various methods for the preparation of metal oxide nanoparticles have been developed with the ultimate goal of producing particles of controllable properties including size distribution, morphology, and crystal structure. Amongst these methods is supercritical fluid drying, where the solvent is removed above its critical temperature (T_c) and critical pressure (P_c). High temperatures have been shown to be necessary in obtaining very fine particles as the liquid-vapour interface and capillary pressure are eliminated and the resulting particles do not tend to stick to each other [8-11].

The synthesis of zinc oxide (ZnO) nanoparticles using various methods has been reported in literature [12-33]. Han *et al* [18] prepared ZnO nanoparticles in supercritical methanol and supercritical water and obtained particles down to 10 nm size. Gao *et al* [19] dried alcoholic ZnO gels by supercritical carbon dioxide drying. Monolithic zinc oxide aerogels were reportedly prepared using supercritical carbon dioxide by Krumm *et al* [20].

1.1. Specific surface area and Pore volume

Previous studies on the surface area and pore volume of ZnO particles prepared with different methods are summarized in Table 1.

"Table 1. Adsorptive properties of nanosized ZnO particles"

Synthesis Method	Surface Area, m^2/g	BJH Pore volume, cm^3/g	BJH Pore diameter, nm	Ref.
Supercritical CO_2 drying	277	0.17	1.54	19
Conventional drying	240	0.30	1.58	19
Supercritical CO_2 drying and annealing at 150^oC	102	0.18	2.99	19
Conventional drying and annealing at 150^oC	95	0.24	2.56	19
Super critical methanol drying at 30 MPa and 400^oC	21.3			16
Zinc acetate thermal decomposition	37		2.5-10	27
Ammonia treated zinc acetate thermal decomposition	60		25% lower than 2.5-10.0	27

Hallow microspheres In supercritical CO_2 and ethanol at 333K and calcined at 777 K	9.3		2-4	30
BioinspiredZnO prepared using egg shell template at pH2 and 450^oC	9.86	0.039	2.84	32
Conventional drying	39.1	0.048		26
Freeze drying at-40^oC and 0.7 Pa	20.1	0.031		26

ZnO aerogel and zinc xerogel were obtained by drying the ZnO gels by supercritical carbon dioxide drying and by conventional methods by Gao *et al* [19]. An increase in pore volume was observed in the xerogel compared to the aerogel (0.30 cm^3/g compared to 0.17cm^3/g respectively). This is most likely a reflection of the difference in the gel morphology. The analogous annealed materials at 150^oC exhibited significantly smaller surface areas (102 m^2/g and 95 m^2/g) compared to the original materials, 277 m^2/g compared to 102m^2/g for the aerogel-based material. In both cases, there is minimal change observed in the pore volume with a dramatic increase in average pore diameter; this is likely a consequence of the aggregation of particles into larger platelets during supercritical carbon dioxide drying [19].

Estruga *et al*[27] synthesized two different types of ZnO by decomposing zinc acetate and ammonia treated zinc acetate by heat. Low-temperature nitrogen adsorption-desorption analysis showed that the materials obtained by both routes had similar textural characteristics. The pore size distribution calculated from the adsorption branch denotes the presence of mesopores in the 2.5-10.0 nm range, which is related to the H2 hysteresis loop. The specific surface area (*S*SA) of zinc oxide obtained from zinc acetate was 37m^2g^{-1}, which increased to 60 m^2g^{-1} for the ZnO obtained by the ammonia route [27].

The BET surface area of hollow ZnO microspheres was 9.3m^2g^{-1}. Microspheres had mesopores (2-4 nm) and large macropores with diameters >20 nm [30]. Bioinspired ZnO synthesized by using egg membranes had surface area of 9.86 m^2g^{-1}, pore volume of 0.039 cm^3g^{-1} and pore size of 2.84 nm [32]. The surface area of conventional dried and freeze dried ZnO were 39.1 and 20.1 m^2/g respectively and the pore volume was also lower for freeze dried ZnO (0.031cm^3/g) than for conventional dried sample (0.038cm^3/g) [26].

1.2. Carbon dioxide adsorption

A complete understanding of the carbon dioxide (CO_2) interaction with zinc oxide (ZnO) is a basis for the development of new ZnO-containing materials for catalytic fixation of CO_2 into useful chemicals such as methanol. The activation of CO_2 by ZnO via the carbonate-ion formation requires the presence of empty surface Zn−O pairs [34].

Noei *et al* [35] have reported that the adsorption of CO_2 on pure ZnO nanoparticles gives rise to three kinds of carbonate species: These are: (i) A tridentate carbonate formed as a majority species on the mixed terminated ZnO (1010) surface (1581 and 1329 cm^{-1}) supported by the fact that the polycrystalline ZnO nanoparticles

are dominated by the non-polar (1010) facets [36]. (ii) A bidentate carbonate formed on the polar O-ZnO surface via the activation of CO_2 on O vacancy sites (1621 and 1292 cm^{-1}). (iii) A monodentate carbonate resulting from CO_2 adsorbed on defect sites and identified as a minority species (1543 and 1313 cm^{-1}). In addition, two weak IR bands appeared at 1543 and 1313 cm^{-1} for the hydroxylated ZnO nanoparticles which are characteristic of polydentate carbonate species formed via the CO_2 activation on defects in the presence of hydroxyl groups [37].

1.3. Light absorption and emission by ZnO

All transmittance spectra of ZnO films show sharp absorption edges in the wavelength region between 370 and 380 nm [28]. Mishra *et al* [24] reported a clear absorbance peak at ~ 374 nm (3.31 eV) and at ~ 376 nm (3.29 eV) for ZnO nanoparticles prepared at 400^{o}C for 3 hours and 12 hours respectively. The luminescence bands of ZnO irradiated with UV light changes with the defects and impurities in ZnO as well as irradiation wavelength. The three main peaks appear at 426 nm, 486 nm and 511 nm, in all the ZnO samples prepared at different pH values and irradiated with 250 nm light [29]. The UV band edge emission centred at 426 nm, broad blue bands centred at 486 nm and green bands centred at 511 nm were observed from the photoluminescence (PL) spectra. The PL signal at 426 nm is a typical near band edge UV emission of ZnO which indicates a direct recombination of excitons through an exciton-exciton collision process. The luminescence blue bands at 486 nm are due to transition vacancy of oxygen and interstitial oxygen. The green emission at 511 nm referred to a deep level emission usually caused by the presence of ionized oxygen vacancy on the surface and results from the recombination of a photo generated hole with a single ionized charged state of the defects in zinc oxide. The ZnO nanoparticles were synthesized in the atmosphere of deficient oxygen, which caused large amounts of oxygen vacancies, so the peak of green emission band is very high. Many past reports on PL emission spectra of ZnO show a broad peak in the green region between 520 nm and 550 nm in case of both bulk zinc oxide as well as quantum dots and similar size features at 420 nm to interstitial oxygen levels in zinc oxide and the feature at 485 nm to the transition between vacancy of oxygen and interstitial oxygen [29]. Highly oxygen deficient ZnO structures had a broad and intense emission in green yellow region due to singly ionized oxygen vacancies [31] when excited with 320 nm UV light.

Generally, visible emission in ZnO consists of blue, violet, green and yellow emission peaks which can be attributed to different intrinsic defects [24]. A weak yellow band is usually observed in ZnO materials just above 600 nm [19]. Reports have shown that the characteristic luminescent spectrum of ZnO exhibits two maxima: around 380 nm (near-UV emission) and 500 nm (green emission) respectively [25]. The former being attributed to the exciton band (band-gap fluorescence caused by a transition from the lower edge of the conduction band to the upper edge of the valence band) recombination while the latter is attributed to the density of singly ionized oxygen vacancies [25]. Tuning of ultra-violet to green emission of ZnO by choosing suitable excitation wavelength was possible [33]. Mir and Ghoul [38] showed that vanadium-doped nanosized zinc oxide aerogel exhibited

strong red emission when excited with 380 nm UV light. The solvent of the ZnO sols and wavelength of the exciting light affected the absorption and emission of the light [35]. The visible green emission is dominant over the UV emission for hollow ZnO microspheres produced by supercritical CO_2 extraction [30]. The as-synthesized aerogel, **A1**, exhibited only weak emission peaks which can be attributed largely to the highly amorphous nature of the unheated sample and small crystallite size. The PL spectrum of the sample annealed at 250 ^oC exhibited observed strengthening in the emission intensity of both the UV and blue emissions, which is likely due to the increased crystalline nature of the annealed samples as revealed by the XRD analysis [30].

There are many studies made with CO_2 [18], water [17] and methanol [16] in supercritical drying of ZnO. However, ethanol which is a cheap and abundant solvent with lower critical pressure than other solvents such as CO_2, water and methanol have not been widely used for supercritical drying of ZnO. In a previous study, we reported on the preparation of ZnO nanoparticles in supercritical ethanol and its use in lubricants [21]. ZnO samples having initially 6.4% water and 36.9% ethanol were dried both with conventional drying at 110^oC and supercritical ethanol drying at 7.2 MPa and 250^oC using a solid liquid ratio of 5g/100cm^3 in a 300cm^3 high pressure reactor. Conventional dried ZnO was called ZnO-A while supercritical ethanol dried ZnO was called ZnO-B in the previous study. The ethanol phase contained only 0.38% water after the supercritical drying process. However, ZnO-B contained 10% ethanol after removal from the supercritical drying system as previously reported, but was evaporated under ambient conditions since no peaks related to ethanol were present in its FTIR transmission spectrum. EDX analysis indicated that the ZnO nanoparticles contained >95% ZnO. However the Zn content (81.1 and 83.3% for ZnO-A and ZnO-B respectively was higher than expected for pure ZnO (76%). The chlorine content, 3.2% of the supercritical ethanol dried sample ZnO-B, was lower than that of the conventionally dried sample, 5.3%. The X-ray diffraction diagrams showed that the nanoparticles having 16.7nm size were transformed to larger particles with 24.7nm size by supercritical ethanol drying. The absence of surface tension of liquid ethanol during supercritical ethanol drying was not sufficient to prevent agglomeration of the particles. Due to very high pressure used in supercritical extraction, the particles obtained were more agglomerated compared to the particles obtained by conventional drying at atmospheric pressure. As part of our continuing studies on ZnO nanoparticles prepared in supercritical ethanol, we report in this study on the optical and surface properties of ZnO nanoparticles prepared in supercritical ethanol in comparism with ZnO nanoparticles produced by conventional method. For this purpose, N_2 and CO_2 adsorption isotherms were determined, dehydration behaviour was examined by *in situ* FTIR spectroscopy, light absorption and emission of the powders were also examined.

2. EXPERIMENTAL METHOD

2.1. Preparation of ZnO nanoparticles

The procedures for the synthesis of ZnO nanoparticles using the conventional method

of drying (ZnO-A) and supercritical ethanol drying (ZnO-B) were as described previously [21]. The sample in the steel reactor was heated to supercritical condition of 7.2 MPa and 250^{o}C and the pressure of the reactor was reduced to 0.01 KPa by opening the valve connecting to a second expansion reactor at room temperature and pressure. The supercritical ethanol dried sample was taken out after cooling the hot reactor to room temperature. Conventional drying was made at 110^{o}C and atmospheric pressure.

2.2. Surface Characterization of ZnO nanoparticles

The adsorptive properties of the synthesized ZnO nanoparticles were measured using ASAP Micromeritics 2000 (Norcross Georgia USA). The nitrogen physisorption isotherms were obtained at 77.35K. Surface areas were evaluated using the Brunauer-Emmet Teller (BET) method from the adsorption branch of the isotherm. The pore size distributions were according to the Barrett-Joyner-Halenda (BJH) model, and the average pore diameters and cumulative pore volumes were calculated using the desorption branch of the isotherm. Before each set of measurements, the samples were degassed for 20-40h. Each measurement took about 24 hours to complete with a 45s equilibrium interval. The measurement of the adsorptive properties (using the BET equation) was carried out using low temperature nitrogen adsorption based on the evaluation of the amount of adsorbate covering the adsorbent with a monolayer (from the adsorption isotherm).

Carbon dioxide (CO_2) adsorption experiments were also conducted on the synthesized ZnO nanoparticles. This analytical method involves studying the interaction of a gas with a substrate surface. The adsorption isotherms of carbon dioxide on ZnO samples at 25^{o}C were measured in the pressure range of 0.1 to 100 KPa using ASAP Micromeritics 2000. The samples were outgassed at 110^{o}C and 0.001 Pa overnight before adsorption experiments.

2.3. *In situ* DRIFT Spectroscopic Measurements

Diffuse Reflectance Fourier Transform Infrared (DRIFT) measurements were carried out in an *in situ* heating reaction cell fitted with CaF_2windows (Harricks, NY) shown in Fig. 1.

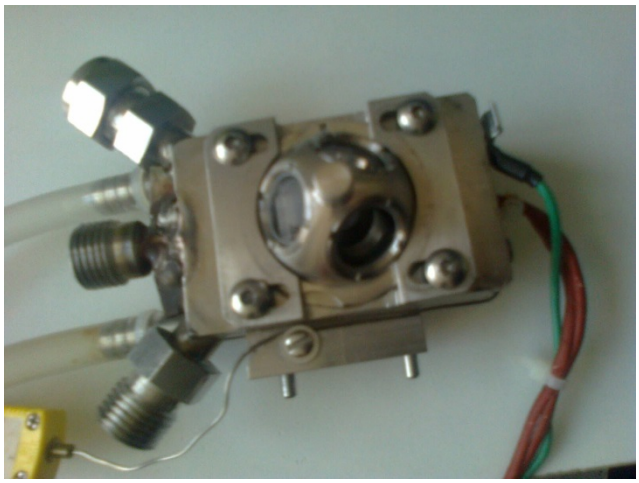

Fig. 1. ***In situ*** **heating cell with atmosphere control (Harricks**)

A praying mantis optical geometry was used to direct the infrared beam. A 0.1g sample was placed on the sample holder and after its spectrum at room temperature and 100 KPa pressure was taken, the sample chamber was evacuated down to the 0.1 Pa pressure and heated up to 500^{o}C at a 2^{o}C min^{-1} rate at0.1Pa pressure. The DRIFT spectrum of the sample was obtained at different temperatures during its dynamic heating.

2.4. Optical Measurements of ZnO aqueous dispersions

Dispersions of ZnO-A and ZnO-B in water were used for optical studies. UV-visible spectra were recorded by using a Perkin Elmer Lambda 45 UV/VIS spectrophotometer (Massachusetts, USA). Room temperature photoluminescence (PL) spectra of the dispersions excited at 280 and 375 nm were obtained by using Varian Cary Eclipse fluorescence spectrometer (Santa Clara California USA).

3. RESULTS AND DISCUSSION

3.1. Characterization of ZnO nanoparticles

ZnO nanoparticles prepared and dried by two methods: conventional (ZnO-A) and supercritical ethanol drying (ZnO-B) have been previously characterized by various analytical methods. These include Fourier Transform Infrared (FT-IR) spectrophotometry, Scanning Electron Microscopy (SEM), X-ray Diffraction (XRD) and Thermogravimetric analysis (TGA) to elucidate the shape, size, composition and stability of the nanoparticles [27].

3.2. Nitrogen Adsorption

The surface areas of the ZnO nanoparticles were determined by recording the nitrogen adsorption/desorption isotherms. Fig. 2 shows the adsorption-desorption isotherms for ZnO-A and ZnO-B.

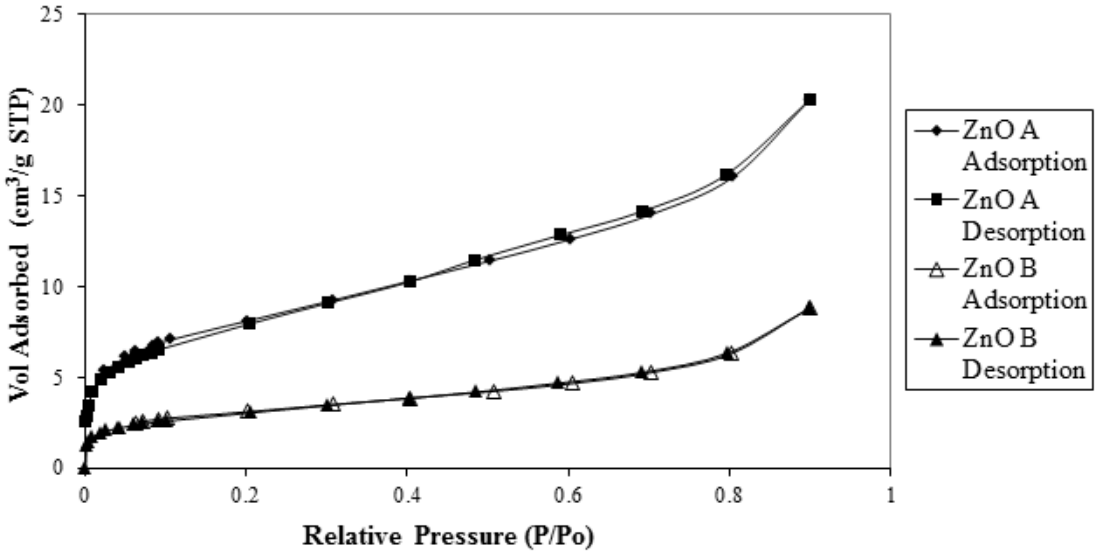

Fig. 2. Nitrogen adsorption-desorption isotherms for (a) ZnO-A (b) ZnO-B

The shape of the isotherm indicates the mesoporous structure of ZnO [23]. There was a steady increase in the amount of nitrogen adsorbed up to a maximum ofp/p_o = 0.9 for both samples. Table 2 summarizes the surface areas, pore volumes and average pore sizes for ZnO-A and ZnO-B. ZnO-A had a larger surface area (BET) 28.3 m^2/g than ZnO-B which had a lower value of 10.61 m^2/g. The particle size of ZnO-A and ZnO-B were found to be 40 and 100 nm respectively from their surface areas. However, using dynamic light scattering on a Zetasizer 3000 HSA, it was found that 95% of the particles were 78.1nm in diameter for ZnO-A and 92% of the particles had an average diameter of 107.7nm for ZnO-B.[21]Supercritical ethanol dried ZnO-B was found to have lower particle size than conventionally dried ZnO-A. By both techniques, the pore size (5.17nm) of ZnO prepared by supercritical ethanol drying (ZnO-B) was larger than that (4.48nm) of conventional dried ZnO (ZnO-A). Also the pore sizes were larger than the ZnO particles prepared by other investigators [16, 19, 27, 30, 32].

Table 2. Adsorptive properties of nanosized ZnO particles prepared in the present study

Synthesis Method	Surface Area, m^2/g	BJH Pore volume, cm^3/g	BJH Pore diameter, nm
Conventionally dried ZnO (ZnO-A)	28.30	0.03	4.47
Supercritical ethanol dried ZnO (ZnO-B)	10.61	0.01	5.17

3.3. Carbon dioxide Adsorption

Fig. 3 shows the CO_2 adsorption isotherms obtained for ZnO-A and ZnO-B. The isotherms in Fig. 3 indicate that the ZnO nanoparticles adsorbed very small amounts of CO_2. The conventionally dried powder adsorbed more CO_2 (0.5 cm_3/g) than supercritical ethanol dried sample (0.34 cm^3/g) at 90 KPa. The CO_2 adsorption at 25^oC was not a physical adsorption. It should have formed carbonates or bicarbonates by interacting with Zn-O or Zn-OH groups [34-36, 38]. Xia *et a*l [39] investigated CO_2 adsorption on ZnO by static adsorption microcalorimetry. They reported that the amount of CO_2 adsorption is dependent on the surface treatment of ZnO. Maximum 5 $\mu mol/m^2$ (1.2 cm^3/g) CO_2 was adsorbed on ZnO with 10 m^2/g surface area at 30^oC which was outgassed at 400^oC for 2 hours under vacuum before adsorption experiments. The lower outgassing temperature or hydration of ZnO surface with water lowered CO_2 adsorption. Since the samples were outgassed at 110^oC in the present study, a lower amount of CO_2 adsorption was observed.

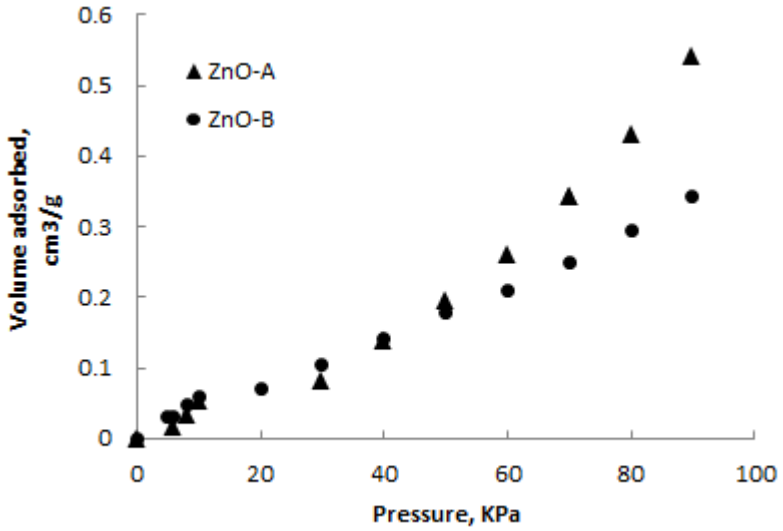

Fig. 3. CO_2 adsorption isotherms for ZnO nanoparticles at 25^oC

3.4. *In situ* Drift FTIR Spectroscopic Measurements

Figs. 4a and 4b presents the DRIFT spectra of the synthesized ZnO nanoparticles under different conditions.

Noei *et al* [40] studied water vapour adsorption on a single crystal of ZnO. The DRIFT spectra obtained before and after exposing the O_2 pre-treatedZnO samples in addition to water at 323 K showed that upon water exposure the features at 3656 and 3639 cm^{-1} disappear, whereas the 3672 cm^{-1} band gains in intensity and becomes the dominant one and the intensity of the bands at 3620 and 3448 cm^{-1} decreases, while the latter shifts to lower frequencies and becomes broader, indicating a H-bond interaction. A new band at 1617 cm^{-1} appears which is characteristic for a water scissoring mode, thus confirming the molecular adsorption of H_2O on ZnO

nanoparticles. The deuteriated water exchange studies indicated that the peaks at 3687, 3672, 3620, 3448 cm^{-1} belonged to H_2O in ZnO, OH on ZnO with co-adsorbed H_2O, OH on ZnO and OH in defect sites respectively [40]. In Fig. 4a, the isolated OH group vibration peaks at 3846, 3736 cm^{-1}decrease in intensity on heating but do not disappear completely, hydrogen bonded OH vibration peak at 3483cm^{-1}decrease in intensity on heating. New peaks at 3547 and 3444 appear at 200^{o} C and decrease in intensity on heating.

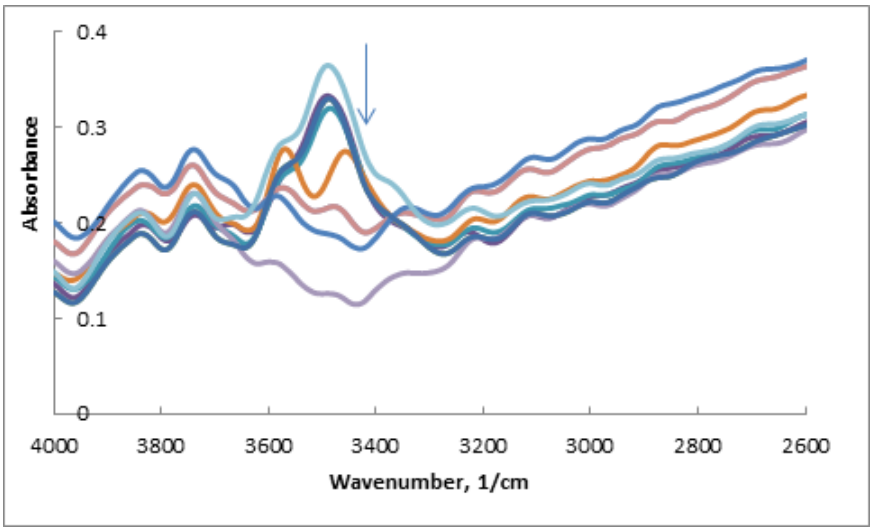

(a)

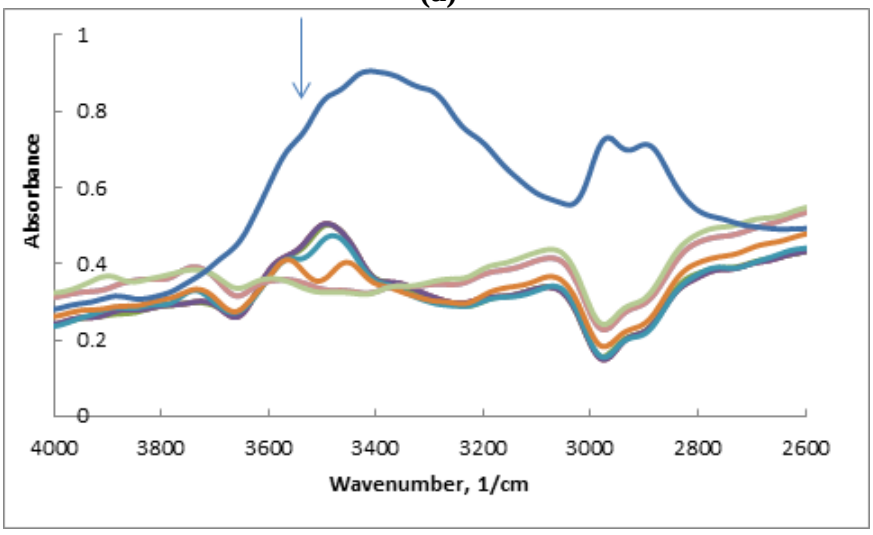

(b)

Fig. 4. DRIFT spectra of (a) Supercritical ethanol dried zinc oxide (ZnO-A) under different conditions in the arrow direction at 25^{o}C and 10 KPa, 25^{o}C and 0.1 Pa, 100^{o}C and 0.1 Pa, 200^{o}C and 0.1 Pa, 300^{o}C and 0.1 Pa, 400^{o}C and 0.1 Pa, 500^{o}C and 0.1 Pa (b) Conventionally dried zinc oxide (ZnO-B) at 25^{o}C and 10 KPa, 25^{o}C and 0.1 Pa, 100^{o}C and 0.1 Pa, 200^{o}C and 0.1 Pa, 300^{o}C and 0.1 Pa, 400^{o}C and 0.1 Pa, 500^{o}C and 0.1 Pa

In Fig. 4b, 3392 cm^{-1} (OH stretching), 2960 and 2883 cm^{-1} (CH_2 asymmetric and symmetric stretching vibrations) peaks belonging to ethanol on the surface of supercritical ethanol dried sample disappear by reducing the pressure to 0.1 Pa. The transmission FTIR spectra of the same samples taken by KBr disc technique indicated there were no peaks related with ethanol in both supercritical ethanol dried and conventionally dried samples [21]. Since transmission and drift spectra give information about the bulk and the surface of a sample, it can be concluded that ethanol was only present at the surface of the supercritical ethanol dried sample. The peak belonging to isolated OH groups at 3728 cm^{-1} in drift spectra had lower intensity for supercritical ethanol dried sample than conventionally dried sample and its intensity lowered to a small extent on heating up to 500°C. The peak at 3485 cm^{-1} for hydrogen bonded OH groups appear by vacuum application at room temperature and decreased in intensity on heating. There are peaks that appear at 200°C at 3554 and 3460 cm^{-1} and disappear at 300°C.

The *in situ* DRIFT study of the samples indicated that in order to obtain pure ZnO by supercritical ethanol drying system, a vacuum pump should be added to the supercritical ethanol drying system to remove the last traces of ethanol from the system.

3.5. Optical Properties of Aqueous Dispersions of ZnO

3.5.1. UV/VIS Spectra

The electronic absorption spectrum of ZnO samples in the UV/VIS range enables the characterization of the absorption edge related to the semiconductor band structure [2]. Fig. 5 shows the UV/VIS absorption spectra of the nanosized ZnO particles.

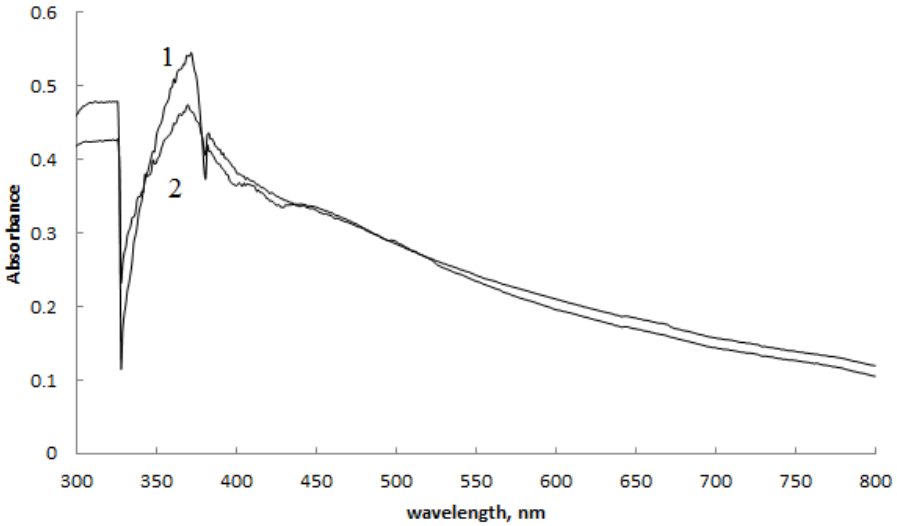

Fig. 5. UV/VIS absorption spectra of the nanosized ZnO particles (1) ZnO-A (2) ZnO-B

The UV/VIS absorption spectra for both ZnO-A and ZnO-B exhibit a very strong UV absorbance peak at ~ 375 nm, and can be attributed to bound exciton

emission [23]. Conventional dried ZnO had a higher absorbance value than supercritical ethanol dried ZnO.

3.5.2. Photoluminescence Measurements

Room temperature photoluminescence (PL) spectroscopic study enables the determination of the electronic energy levels from where emission is particularly observed, which in turn helps to corroborate the band structure of the ZnO nanoparticles.[2] The results of the PL spectrum for the synthesized ZnO nanoparticles are presented in Figs. 6 and 7.

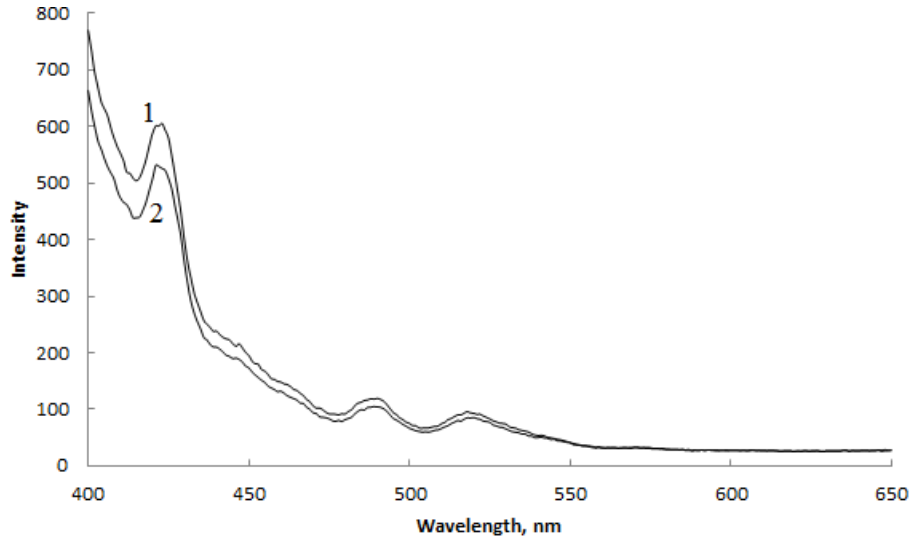

Fig. 6. Luminescence spectrum of ZnO exited by 375 nm UV light (1) ZnO-A (2) ZnO-B

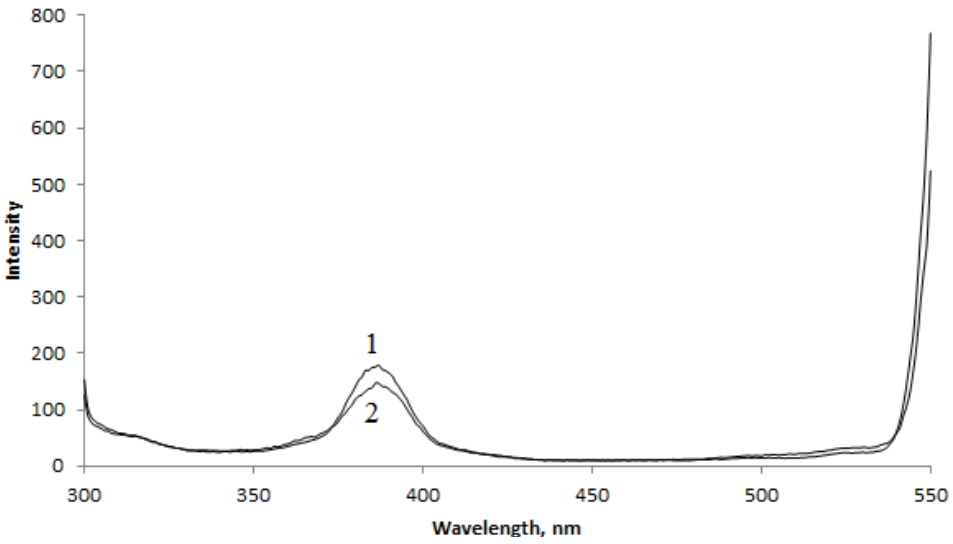

Fig. 7. Luminescence spectrum of ZnO irradiated with 280 nm UV light (1) ZnO-A (2) ZnO-B

The samples excited at different wavelengths of UV light had different luminescence spectra as in the study of Chen and Zang [41]. The PL spectra of the ZnO nanoparticles at excitation wavelength of 280 nm at room temperature exhibits a UV emission peak at 386 nm (~3.11eV) and 550 nm. The UV emissions band at 386 nm is related to near band-edge (NBE) emission of the ZnO nanoparticles and is attributed to the recombination of the free excitons by exciton-exciton collision process.[25] At excitation wavelength of 375 nm, broad visible emission peaks including violet emission at ~424 nm (~2.96eV), blue-green emission at ~ 490 nm (~2.56 eV) and green emission at ~ 520 nm (~2.37eV) were observed. The emission at 426 nm is due to transition vacancy oxygen and interstitial oxygen. [29] The peak at 486 nm is deep level emission due to photogenerated hole with single ionized charge [2]. The peak at 511 nm is due to singly ionized oxygen vacancy [24, 25]. The luminescence intensity of supercritical ethanol dried ZnO (ZnO-B) had lower values than that of conventionally dried ZnO (ZnO-A).

4. CONCLUSION

The surface and optical properties of ZnO nanoparticles prepared and dried by conventional drying (ZnO-A) and supercritical ethanol drying (ZnO-B) have been studied. The mesoporous nanoparticles of supercritical ethanol dried zinc oxide had lower surface area (10.61 m^2/g) than that of conventionally dried ZnO (28.30 m^2/g) due to increase of the particle size under supercritical conditions. The powders adsorbed very small amount of CO_2 and the conventionally dried powder adsorbed more CO_2 (0.5 cm^3/g) than supercritical ethanol dried sample (0.34 cm^3/g) at 90 KPa. Supercritical ethanol dried ZnO (ZnO-B) had ethanol on its surface which was eliminated by vacuum application at room temperature. Thus, the ethanol supercritical set up should be improved by adding a vacuum line to the reactor. This would ensure that the sample is successfully cleaned from ethanol after cooling to room temperature. Both powders had OH groups which were eliminated on heating up to 500 ^oC under vacuum. However, OH groups were present in lower amounts in supercritical ethanol dried ZnO. UV-visible absorption spectrum of both powders had an excitonic peak at 375 nm. The photoluminescence (PL) spectra for both samples show emission peaks such as NBE, violet, blue-green and green emissions. Luminescence intensity of supercritical ethanol dried ZnO (ZnO-B) was lower than that of conventionally dried ZnO (ZnO-A).

ACKNOWLEDGEMENTS

The authors acknowledge using the laboratory facilities of Izmir Institute of Technology (IZTECH), Turkey.

References

[1] E. Tang, G. Cheng, X. Ma, X. Pang, Q. Zhao, Surface modification of zinc oxide nanoparticle by PMAA and its dispersion in aqueous system, Appl. Surf. Sci. 252 (2006) 5227-5232.

[2] S. Dutta, N. Ganguly, Characterization of ZnO nanoparticles grown in presence of Folic acid template, J. Nanobiotechnology 10 (2012) 29-38.

[3] R.Y. Hong, J.H. Li, L.L. Chen, D.O. Liu, H.Z. Li, Y. Zheng, J. Ding, Synthesis, surface modification and photocatalytic property of ZnO nanoparticles, Powder Technol. 189 (2009) 426-432.

[4] S.F. Wang, J.M. Zhang, L.Y. Chen, K.W. Xu, Influences of Cd-substitution and intrinsic vacancies on the electronic structures and optical properties of ZnO nanotubes, J. Supercond. Nov. Magn. 25 (2012) 2457-2463.

[5] C.Y. Tsay, W.C. Lee, Effect of dopants on the structural, optical and electrical properties of sol-gel derived semiconductor thin films, Curr. Appl. Phys. 13 (2013) 60-65.

[6] M. Gönen, D. Balköse, R.B. Gupta, S. Ülkü, Supercritical carbon dioxide drying of methanol-zinc borate mixtures, Ind. Eng. Chem. Res. 48 (2009) 6869-6876.

[7] B. Wang, W. Zhang, W. Zhang, C. Yu, G. Wang, L. Huang, A.S. Mujumdar, Influence of drying processes on agglomeration and grain diameters of Magnesium oxide nanoparticles, Dry. Technol. 25 (2007) 715-721.

[8] R. Viswanathan, G. Daniel Lilly, W.F. Gale, R.B. Gupta, Formation of Zinc Oxide-Titanium Dioxide Composite Nanoparticles in Supercritical Water, Ind. Eng. Chem. Res. 42 (2003) 5535-5540.

[9] A.S. Mujumdar, L.X. Huang, Global R & D needs in drying, Dry. Technol. 25 (2007) 647-658.

[10] Y. Masmoudi, A. Rigacci, P. Ilbizian, F. Cauneau, P. Achard, Diffusion during the supercritical drying of silica gels, Dry. Technol. 24 (2006) 1121-1125.

[11] T. Tachiwaki, Supercritical fluid drying of aqueous 2-propanol suspension, Dry. Technol. 22 (1 & 2) (2004) 324-334.

[12] T. Tsuzuki, P.G. McCormick, ZnO nanoparticles synthesised by mechanochemical processing, Scripta mater. 44 (2001) 1731-1734.

[13] J. Wang, L. Gao, Synthesis and characterization of ZnO nanoparticles assembled in one-dimensional order, Inorg. Chem. Commun. 6 (2003) 877-881.

[14] J. Merchant, M. Cocivera, Preparation and Doping of Zinc Oxide Using Spray Pyrolysis, Chem. Mater. 7 (1995) 1742-1749.

[15] A.N. Tsvigunov, A New Modification of Zinc Oxide Synthesized by the Hydrothermal Method. Glass Ceram, 58 (7-8) (2001) 280-282.

[16] B. Veriansyah, J.D. Kim, B. Koun, M.Y. Ho, S. Youn-Woo, L.K. Kim, Continuous synthesis of surface-modified zinc oxide nanoparticles in supercritical methanol, J. Supercrit. Fluid. 52 (2010) 76-83.

[17] R. Viswanathan, R.B. Gupta, Formation of zinc oxide nanoparticles in supercritical water. J. Supercrit. Fluid. 27 (2003) 187-193.

[18] N.S. Han, H.S. Shim, J.H. Seo, S.M. Park, B.K. Min, Optical properties and lasing of ZnO nanoparticles continuously in supercritical fluids, Chem. Phys. Lett. 505 (2011) 51-56.
[19] Y.P. Gao, C.N. Sisk, L.J. Hope-Weeeks, A sol-gel route to synthesize monolithic zinc oxide aerogels, Chem. Mater. 19 (2007) 6007-6011.
[20] M. Krumm, C.L. Pueyo, S. Polarz, Monolithic zinc oxide aerogels from organometallic sol-gel precursors, Chem. Mater. 22 (18) (2010) 5129-5136.
[21] T.O. Egbuchunam, D. Balkose, Effect of supercritical ethanol drying on the properties of zinc oxide nanoparticles, Dry. Technol. 30 (7) (2012) 739-749.
[22] T. Jesionowski, A. Kołodziejczak-Radzimska, F. Ciesielczyk, J. Sójka-Ledakowicz, J. Olczyk, J. Sielski, Synthesis of Zinc Oxide in an Emulsion System and its Deposition on PES Nonwoven Fabrics, Fibres Text. East. Eur. 19 (85) (2011) 70-75.
[23] H. Zhang, G. Chen, G. Yang, J. Zhang, X. Lu, Optical properties of amorphous/crystalline ZnOnano-powder prepared by solid state reaction, J. Mater. Sci: Mater Electron 18 (2007) 381-384.
[24] S.K. Mishra, R.K. Srivastava, S.G Prakash, ZnO nanoparticles: Structural, optical and photoconductivity characteristics, J. Alloy Compd. 539 (2012) 1-6.
[25] Z. Guo, S. Wei, B. Shedd, R. Scaffaro, T. Pereira, H.T. Hahn, Particle surface engineering effect on the mechanical, optical and photoluminescent properties of ZnO/vinyl-ester resin nanocomposites, J. Mater. Chem. 17 (2007) 806-813.
[26] C.P. Rezende1, J.B. Da Silva, N.D.S. Mohallem, Influence of Drying on the Characteristics of Zinc Oxide Nanoparticles, Braz. J. Phys. 39 (1A) (2009) 249.
[27] M. Estruga, C. Domingo, J.A. Ayllón, Mild Synthetic Routes to High-Surface Zinc Oxide Nanopowders, Eur. J. Inorg. Chem. 2010 (11) (2010) 1649-1654.
[28] S. Ohara, T. Mousavand, *et al.* Continuous production of fine zinc oxide nanorods by hydrothermal synthesis in supercritical water, J. Mater. Sci. 43 (7) (2008) 2393-2396.
[29] P. Chand, A. Gaur, A. Kumar, Structural and optical properties of ZnO nanoparticles synthesized at different pH values, J. Alloy Compd. 539 (2012) 174-178.
[30] K. Matsuyama, K. Mishima, T. Kato, K. Ohara, Preparation of Hollow ZnO Microspheres Using Poly (methyl methacrylate) as a Template with Supercritical CO_2-Ethanol Solution, Ind. Eng. Chem. Res. 49 (18) (2010) 8510-8517.
[31] N.K. Sing, S. Shirivasta, S. Rath, S. Annapoorni, Optical and room temperature properties of highly oxygen deficient flower like ZnO nanostructures, Appl. Surf. Sci. 257 (2010) 1544-1549.
[32] Q. Dong, H. Su, *et al.* Fabrication of hierarchical ZnO films with interwoven porous conformations by a bioinspiredtemplating technique, Chem. Eng. J. 137 (2) (2008**)** 428-435.
[33] L.R. Singh, R.S. Ningthoujam*et al.* Tuning of ultra-violet to green emission by choosing suitable excitation wavelength in ZnO: Quantum dot, nanocrystals and bulk, J. Alloy Compd. 487 (1-2) (2009) 466-472.

[34] Q.Tang, Q. Luo, Adsorption of CO_2 at ZnO: A Surface Structure Effect from DFT+U Calculations, J. Phys. Chem. C. 117 (2013) 22954−22966.

[35] H. Noei, L. Jin, H. Qiu, M. Xu, Y. Gao, J. Zhao, M.Kauer, C. Woll, M.Muhler,Y. Wang, Vibrational spectroscopic studies on pure and metal-covered metal oxide surfaces, Phys. Status Solidi B 250, No. 6, (2013) 1204-1221.

[36] H. Noei, C. Woll, M. Muhler, Y. Wang, Activation of Carbon Dioxide on ZnO Nanoparticles Studied by Vibrational Spectroscopy, J. Phys. Chem. C. 115 (2011)908.

[37] L. El Mir, J. El Ghoul *et al.* Synthesis and luminescence properties of vanadium-doped nanosized zinc oxide aerogel, Phys. B: Condens. Matter 403 (10-11) (2008) 1770-1774.

[38] H. Wilmer, M. Kurtz, K. V. Klementiev, O. P. Tkachenko, W. Gru¨nert, O. Hinrichsen, A. Birkner, S. Rabe, K. Merz,M. Driess, Ch. Wo¨ll, and M. Muhler, Methanol synthesis over ZnO: A structure-sensitive reaction Phys. Chem. Chem. Phys. 5 (2003) 4736.

[39] X. Xia, J. Strunk, W. Busser, R.N. d'Alnoncourt, M. Muhler, Probing the Surface Heterogeneity of Polycrystalline Zinc Oxide by Static Adsorption Microcalorimetry. 1. The Influence of the Thermal Pretreatment on the Adsorption of Carbon Dioxide,*J. Phys. Chem. C.* 2008, 112, 10938.

[40] H. Noei, H. Qiu, Y. Wang, E. Loffler, C. Woll, M.Muhler, The identification of hydroxyl groups on ZnO nanoparticles by infrared spectroscopy, Phys. Chem. Chem. Phys., 10 (2008) 7092-7097.

[41] Q.H. Chen, W.G. Zhang, Continuous preparation of decorated nano zinc oxide organic sols with intense luminescence, J. Non-Cryst. Solid 353 (4) (2007) 374-378.